



Published in final edited form as:

*Gene Ther.* 2017 March ; 24(3): 187–198. doi:10.1038/gt.2016.88.

## Evidence for the in vivo safety of insulated foamy viral vectors

Diana L. Browning<sup>1</sup>, Elizabeth M. Everson<sup>2</sup>, David J. Leap<sup>2</sup>, Jonah D. Hocum<sup>2</sup>, Hao Wang<sup>3,4</sup>, George Stamatoyannopoulos<sup>3</sup>, and Grant D. Trobridge<sup>1,2</sup>

<sup>1</sup>School of Molecular Biosciences, Washington State University, Pullman, WA, USA

<sup>2</sup>Department of Pharmaceutical Sciences, Washington State University, Spokane, WA, USA

<sup>3</sup>Department of Medicine, Division of Medical Genetics, University of Washington, Seattle, WA, USA

### Abstract

Retroviral vector mediated stem cell gene therapy is a promising approach for the treatment of hematopoietic disorders. However, genotoxic side effects from integrated vector proviruses are a significant concern for the use of retroviral vectors in the clinic. Insulated foamy viral (FV) vectors are potentially safer retroviral vectors for hematopoietic stem cell gene therapy. We evaluated two newly identified human insulators, A1 and A2 for use in FV vectors. These insulators had moderate insulating capacity and higher titers than previously developed insulated FV vectors. The A1 insulated FV vector was chosen for comparison with the previously described 650cHS4 insulated FV vector in human cord blood CD34<sup>+</sup> repopulating cells in an immunodeficient mouse model. To maximize the effects of the insulators on the safety of FV vectors, FV vectors containing a highly genotoxic spleen focus forming virus (SFFV) promoter was used to elicit differences in genotoxicity. In vivo, the A1 insulated FV vector showed an approximate 50% reduction in clonal dominance compared to either the 650cHS4 insulated or control FV vectors, although the transduction efficiency of the A1 insulated vector was higher. This data suggests that the A1 insulated FV vector is promising for future pre-clinical and clinical studies.

### Keywords

gene therapy; foamy virus vector; insulator; genotoxicity; hematopoietic stem cell

## INTRODUCTION

Inherited and acquired genetic disorders of the blood affect millions of people. For many hematopoietic diseases, stem cell transplantation is the current standard of care. Finding a matched donor is often not possible and graft versus host disease is a common and severe

Users may view, print, copy, and download text and data-mine the content in such documents, for the purposes of academic research, subject always to the full Conditions of use: [http://www.nature.com/authors/editorial\\_policies/license.html#terms](http://www.nature.com/authors/editorial_policies/license.html#terms)

Correspondence: Grant D. Trobridge, Washington State University, Department of Pharmaceutical Sciences, PO Box 1495, Spokane WA 99210-1495, USA [grant.trobridge@wsu.edu](mailto:grant.trobridge@wsu.edu).

<sup>4</sup>current address: Altius Institute for Biomedical Sciences Seattle, WA 98121.

### CONFLICT OF INTEREST

The authors declare no conflict of interest.

side effect.<sup>1</sup> A promising alternative is to deliver a therapeutic transgene to the patient's own hematopoietic stem cells (HSCs) using retroviral vectors. The use of autologous HSCs avoids the potential for graft versus host disease and retroviral vectors can be used to permanently deliver a therapeutic transgene. Current retroviral vectors used for HSC gene therapy have been extensively modified from their respective parent viruses to improve safety and efficacy, while maintaining the ability to integrate into the host cell genome. The stable genetic delivery of a therapeutic transgene to the HSC allows for expression of the transgene in all mature blood cells allowing for therapeutic correction in any hematopoietic lineage. HSC gene therapy has already been successful in numerous pre-clinical and clinical trials.<sup>2-7</sup>

Unfortunately, severe vector-mediated genotoxic side effects have been observed in clinical trials, including the development of leukemia.<sup>8-10</sup> The integrated retroviral vector provirus has the potential to interact with the host genome via several mechanisms that include enhancer mediated activation of nearby genes.<sup>11</sup> Thus far leukemogenesis has only been observed in clinical trials utilizing gammaretroviral vectors,<sup>8-10</sup> though evidence of genotoxicity has also been observed when lentiviral vectors were used.<sup>6</sup> In a gene therapy trial for  $\beta$ -thalassemia, a dominant clone with a lentiviral vector integration near *HMGA2* causing transcriptional activation was found in one patient. The dominant clone with the integration was restricted to the myeloid lineage and the therapeutic effect was only observed in the erythroid cells. In this context, the integrated vector provirus has not led to malignancy as of this time. Lentiviral mediated genotoxicity has also been observed in pre-clinical studies.<sup>12-14</sup> Vector-mediated clonal expansion was also observed in gammaretroviral gene therapy trials for chronic granulomatous disease which did lead to malignancy.<sup>9, 15, 16</sup> In summary, numerous clinical trials have shown that integrated vector proviruses are capable of dysregulating the host genome which is of significant concern for use in the clinic.

Foamy viral (FV) vectors are a potentially safer alternative for HSC gene therapy.<sup>17-20</sup> Similar to other retroviral vectors, FV vectors integrate in the host cell genome and have been extensively engineered to improve their safety.<sup>21, 22</sup> FV vectors have a potentially safer integration profile,<sup>17, 23, 24</sup> integrating less frequently near transcription start sites (TSS) than gammaretroviral vectors, and less often within genes compared to lentiviral vectors. In addition, both gamma and lentiviral vectors are prone to inefficient transcriptional termination and read-through transcription, which is not readily detectable from integrated FV vectors.<sup>25</sup> FV vectors have reduced genotoxicity when directly compared to gammaretroviral vectors in the 32D genotoxicity assay<sup>19</sup> and reduced prevalence of clonally expanded severe combined immunodeficient (SCID) repopulating cells (SRC) in vivo compared to lentiviral vectors.<sup>20</sup> Importantly, FV vectors efficiently transduce human SRC<sup>21, 26</sup> and in a direct comparison to lentiviral vectors in the dog large animal model FV vectors led to similar marking levels in long term repopulating cells.<sup>27</sup>

Although FV vectors appear to be relatively safe, the promoter used to express the therapeutic gene cassette still has the potential to interact with and dysregulate nearby genes. Though the use of non-promiscuous and weaker promoters would be the preference for gene therapy, therapeutic efficacy may not be possible without the use of an enhancer containing

promoter for some disorders. Current therapeutic attempts for  $\beta$ -thalassemia and leukocyte adhesion disorders were more successful when a strong enhancer containing promoter was utilized.<sup>14, 28–33</sup> Therefore, to further improve safety, retroviral vectors with chromatin insulators are also being developed.<sup>14, 19, 34, 35</sup> Chromatin insulators are genetic elements which prevent inappropriate regulation of gene transcription<sup>36–41</sup> and are used throughout the human genome to regulate gene expression. They can either prevent gene silencing by promoting the opening of condensed chromatin,<sup>42</sup> or block enhancers from interacting with promoters. Enhancer-promoter blocking insulators can cause changes in the chromatin architecture<sup>41, 43</sup> or directly interact with enhancer proteins to prevent enhancer mediated activation of promoters.<sup>40</sup> When an enhancer-promoter blocking insulator is used to flank a therapeutic gene cassette, the therapeutic gene enhancer-promoter is prevented from interacting with the surrounding genome.<sup>34, 44, 45</sup>

Previously we evaluated four insulators from the literature<sup>46, 47</sup> for insulator activity, effects on FV vector titer, and retention in the FV long terminal repeat (LTR) during reverse transcription and integration.<sup>19</sup> We successfully developed a high titer FV vector insulated with a 650 bp version of the chicken hypersensitivity site four insulator (650cHS4) described by Arumugam et al.<sup>46</sup> We also showed that the 650cHS4 reduced the number of hotspots in human CD34<sup>+</sup> cells after 10 days of culture with vectors containing the spleen focus forming virus (SFFV) promoter controlling the transgene. This highly genotoxic enhancer containing promoter increases genotoxicity to allow comparison of vector safety.<sup>48, 49</sup> Liu et al. identified several promising insulators from the human genome by combining bioinformatics and chromatin immunoprecipitation with DNA sequencing (ChIP-seq) and characterized these insulators using in vitro and in vivo assays.<sup>50</sup> Two of these insulators, A1 from human chromosome 1 and A2 from human chromosome 19, are smaller than the 650cHS4 and were shown to have more insulating activity than the full length cHS4 in an antibiotic resistance based insulator activity assay.<sup>50</sup> Here we report the development of novel insulated FV vectors with these newly identified A1 and A2 insulators from the human genome. We also evaluated the efficacy of an A1 insulated FV vector, with the 650 bp cHS4 insulated FV vector, and uninsulated FV vectors in SRCs. These FV vectors also contain the SFFV promoter to maximize the potential effects of an uninsulated FV vector. The effects of insulated FV vectors on the engraftment of vector exposed human CD34<sup>+</sup> cord blood cells, lineage-specific marking, and clonal expansion of vector transduced long term repopulating cells were compared.

## RESULTS

### Development of A1 and A2 insulated FV vectors

Since our previous description of insulated FV vectors, additional efforts have been made to identify novel insulators.<sup>50–54</sup> These efforts have focused on discovering binding sites for the protein CCCTC-binding factor (CTCF), the only protein so far found to be necessary for enhancer blocking insulator activity. Recently Liu et al. described and characterized the enhancer blocking activity of numerous CTCF binding sites from within the human genome.<sup>50</sup> Of these, A1, an insulator from chromosome 1, and A2, an insulator from chromosome 19, were characterized as strong insulators with higher activity than cHS4.

They were also shown to reduce the genotoxicity of gammaretroviral vectors in 32D cells while having no effect on the titer of lentiviral vectors. These insulators are promising candidates for FV vectors. A1 and A2 insulators were positioned in the same position of the 3' LTR U3 of replication incompetent FV vectors (FVSGW-A1 and FVSGW-A2) as previously described for a 650cHS4 insulated FV vector (Figure 1a).<sup>19</sup> These A1 and A2 insulated FV vectors were developed with insulators in both the forward (-F) or reverse (-R) orientation. Positioning of the insulator in the U3 LTR takes advantage of retroviral reverse transcription to copy the insulator from the 3' LTR to the 5' LTR. The final integrated therapeutic vector provirus thus has an internal transgene cassette flanked by insulators.

### A1 and A2 are promising insulators for FV vectors

We used three previously described rapid in vitro assays<sup>19</sup> to compare the efficacy of the A1 and A2 insulators for use in FV vectors. The first assay is a plasmid based enhancer blocking activity assay designed to evaluate the relative enhancer blocking activity of the insulators. The A1 and A2 insulators were directly compared to the previously evaluated 650cHS4 insulator. For this assay, a dual fluorescence enhancer blocking test plasmid was used to compare insulator activity (Figure 1b).<sup>19</sup> An insulator placed in the test position of this plasmid reduces the expression of mCherry by blocking the CMV enhancer (CMVe) activity on the CMV minimal promoter (CMVmin). A copy of the full 1.2 kbp cHS4 was positioned 3' of the mCherry cassette to decrease the effects of the enhancer and increase the effects of the test insulator. A constitutively active EGFP cassette was placed between the CMVe and the 1.2 kbp cHS4 to act as a control for transfection efficiency. Once normalized, the mCherry expression of insulated and uninsulated plasmids can be directly compared and the reduction in fluorescence determined (Supplemental Figure S1a).<sup>19</sup> For comparison, an enhancer blocking activity assay test plasmid with the CMVe removed has also been tested. The CMVe has transactivation activity in 293A cells<sup>55</sup> and most likely has an enhancing effect on the PGK promoted expression of EGFP that is not present in the enhancerless plasmid. This may cause the EGFP normalized baseline expression of mCherry to be artificially high. We have therefore also supplied the percent of mCherry expression based on the non-EGFP normalized MFI and present all data as percent of promoter activity. The A1 and A2 insulators had similar activity regardless of the orientation (Figure 1c). The A1 and A2 insulators were compared to the 650cHS4 using previously reported data for the 650cHS4.<sup>19</sup> The A1 and A2 insulators in the plasmid based assay were significantly stronger than a forward oriented 650cHS4 (60% and 53% of promoter activity compared to 80%) as previously reported<sup>50</sup>, however the activities of A1 and A2 were not significantly different than a reverse oriented 650cHS4. To further investigate the potential effect of the insulators in an FV vector, the A1 and A2 insulators were tested in the context of a FV LTR. The 3' LTRs from FVSGW-A1 (F and R) and FVSGW-A2 (F and R) were tested for insulating activity (Figure 1c). The insulated FV LTRs were positioned so that the CMV enhancer is upstream of the U3 to simulate an integrated FV vector with an enhancer element that could interact with the CMV minimal promoter. Both the A1 and A2 insulators had similar activity when in the FV LTR (~64% of promoter activity), and the difference between A1 and A2 was not significant. In the context of the FV LTR, the A1 and A2 were not as strong as the 650cHS4 insulator.

The production of high titer insulated FV vectors is critical for clinical use. The FVSGW-A1 and FVSGW-A2 insulated FV vectors with the insulators in both forward and reverse orientation were thus compared to determine their titer. Titer was determined on HT1080 human fibroblasts following production in HEK293T human fibroblasts as previously described.<sup>19</sup> Unlike the 650cHS4, the A1 and A2 insulators did not significantly or statistically reduce the titer of FV vectors, regardless of orientation (Figure 1d). FV vectors A1 in the reverse orientation did have lower titers ( $p=0.068$ ) (Supplemental Figure S2).

Since enhancer elements can act bi-directionally, the insulators within the 3' LTR should be retained and accurately copied to the 5' LTR during reverse transcription to be fully effective. Utilizing a shuttle vector rescue approach, we previously showed that strong insulators with repeated insulator elements had a high frequency of recombination causing a reduced number of insulator elements in the final integrated proviruses.<sup>19</sup> To evaluate the retention and fidelity of copying of the A1 and A2 insulators from the 3' LTR to the 5' LTR, these vectors were also assessed for insulator fidelity by shuttle vector rescue as previously described.<sup>19</sup> For this approach, a bacterial origin of replication and kanamycin rescue cassette were added to the new A1 and A2 insulated FV vectors. Following transduction of HT1080 cells, DNA can be extracted and cut into smaller fragments with *NdeI* which cleaves the cell genome but not the vector, and those fragments are then circularized into plasmids that are transformed into *Escherichia coli*. Circularized fragments containing vector genomes are selected for, and the LTRs sequenced.<sup>19</sup> Similar to 650cHS4, the A1 and A2 were present in all captured proviruses in both the 3' LTR and 5' LTR. This shows that both the A1 and A2 insulators are retained and efficiently copied during reverse transcription and integration.

### A1 insulated FV vectors are effective in vitro

Both the A1 and A2 insulators are promising insulators for FV vectors. The vectors have similar insulating activity, do not significantly affect titer, and are retained after integration. Although the difference was not significant compared to A2, the A1 insulator did have the highest insulating activity in the context of the LTR and in the forward orientation did not affect FV vector titer. Therefore, FVSGW-A1-F was further evaluated in human CD34<sup>+</sup> cord blood cells. Previously, we assessed over 10 000 retroviral vector integration sites (RIS) from human CD34<sup>+</sup> cord blood cells cultured in vitro for five or ten days.<sup>19</sup> Cells were transduced with dialyzed FVSGW, FVSGW-650cHS4-R, or FVSGW-A1-F at a target MOI of 10. At five days post vector exposure the transduction frequencies were 9.1%, 11.1%, and 26.8% for FVSGW, FVSGW-650cHS4-R, and FVSGW-A1-F respectively as determined by EGFP expression (Supplemental Figure S1b). Retroviral integration sites were recovered from the DNA of cells harvested at five and ten days post vector exposure. A minimum of 904 unique integration sites for each vector were captured and used to determine the integration profiles. FVSGW-650cHS4-R had a similar integration profile to FVSGW but had significantly fewer integrations within 50 kbp sized hotspots retrieved from five or ten days post vector exposure.<sup>19</sup> We compared the FVSGW-A1-F to both FVSGW-650cHS4-R and the control uninsulated FVSGW (Table 1; Figure 2a). Unexpectedly, we found that FVSGW-A1-F does have a significantly different integration profile compared to both uninsulated FVSGW and to FVSGW-650cHS4-R. The greatest difference between the

integration profile of FVSGW-A1-F and the other foamy viral vectors was observed within the first 1 000 basepairs upstream of gene TSSs, statistical differences ( $p < 0.01$ ) were also seen at other intervals. Similar to our previous study,<sup>19</sup> the in vitro cultures were highly polyclonal and clonal dominance was not apparent for any vector.

The percentage of EGFP expressing cells (marking) for FVSGW and FVSGW-650cHS4-R was less than for FVSGW-A1-F at the time of harvest and fewer unique integrations were captured. Therefore, hotspots were defined as two integrations within 10 kbp<sup>56</sup> and were determined from at least three non-overlapping matched sized samples of 300 RIS, the size of the smallest data set. No significant difference in hotspots was observed, likely due to a relatively low number of RIS (Figure 2b).

### **Insulated vectors do not affect engraftment of or lymphocyte differentiation from SCID repopulating cells (SRC)**

The goal of these studies is to develop a safer insulated retroviral vector gene therapy vectors for use in a clinical setting. Thus we wanted to explore genotoxicity in engrafted clinically relevant human CD34<sup>+</sup> cord blood cells. We thus explored the efficacy and safety of insulated FV vectors in human repopulating cells in an immunodeficient mouse model. We utilized the well-established non-obese diabetic SCID gamma (NSG) mouse model to explore the safety of insulated FV vectors in vivo. These mice are severely immunocompromised and allow for human stem cell engraftment and hematopoiesis. In order to maximize the effects of the insulators on the safety of FV vectors, FV vectors containing a SFFV promoter controlling the expression of EGFP were used. Our rationale was that in order to compare the relative safety of insulated and uninsulated FV vectors in normal human CD34<sup>+</sup> cells, within the relatively short time span of repopulating cells in mice, a highly genotoxic promoter would be the most efficient way to elicit differences in genotoxicity. A major advantage of this model over tumor prone mouse models is that genotoxicity is evaluated in normal human cord blood CD34<sup>+</sup> cells.

Vector exposed human cord blood CD34<sup>+</sup> cells were intravenously transplanted into myeloablated four week old NSG mice. At six weeks post-transplant, marked human CD45<sup>+</sup> cells were already present in the blood (~35%) of all transplanted mice regardless of vector treatment (Figure 3a). Engraftment in all mice was very similar and stabilized to greater than 85% after the 15<sup>th</sup> week post transplantation. Bone marrow taken at weeks 18 and 27 post transplantation also showed similar engraftment of SRCs with greater than 75% of all cells expressing human CD45 (Supplemental Figure S3a). Marking in the peripheral blood also stabilized in all transplanted mice after week 15 (Figure 3b). Marking in the bone marrow at weeks 18 and 27 showed similar average percent marking compared to the peripheral blood (Supplemental Figure S3b). There was a considerable difference in the levels of marking observed in each treatment group that closely matched the final multiplicity of infection (MOI) used for each arm. Although we attempted to use an identical vector dose for all three groups, the MOIs were 6.5 (FVSGW), 10 (FVSGW-650cHS4-R) and 17 (FVSGW-A1-F) due to variability in dialysis of the vector preparations at the time of vector exposure. Marking in human peripheral blood leukocyte lineages was also assessed at 18 and 27 weeks

post-transplant. There was multi-lineage marking with all insulators and no evidence of any lineage-specific effects of the A1 or 650cHS4 insulator (Figure 3c,d).

### Effects of insulators on SCID repopulating cells (SRCs)

In clinical trials for retroviral vector gene therapy, the development of genotoxicity can take years. In our model the genotoxic SFFV promoter was used to accelerate the process of genotoxicity, allowing us to observe differences within the lifespan of immunodeficient mice. We thus evaluated FV vector safety by looking carefully at the distribution and contribution of RIS in the bone marrow and spleens of the transplanted mice. Similar numbers of unique RIS were captured from both live bone marrow aspirates at 18 weeks post transplantation and from bone marrow retrieved following sacrifice at 27 weeks post-transplant. More than 250 total unique integrations from each transplant group were captured (Supplemental Table S1). At 18 weeks the unique integration profile of the different vectors is similar while at 27 weeks the profiles of the FVSGW and FVSGW-650cHS4-R transduced SRCs are further reduced in immediate proximity to TSS (Figure 4a). Similar to the liquid cultures, though, FVSGW-A1-F has reduced integrations within 50 kbp of TSS and within genes and near TSS of proto-oncogenes compared to FVSGW and FVSGW-650cHS4-R (Table 2).

The unique integrations were further assessed for the frequency with which each unique integration was retrieved and the total of different read lengths captured (spans). During the processing for modified genomic sequencing-polymerase chain reaction (MGS-PCR), extracted DNA is acoustically sheared which results in random cutting of the DNA. When clones expand from a cell with a single integrated provirus, each fragment from different cells with the provirus-chromosome junction will have a different distance from the shear site to the LTR. During processing unique sized fragments, or spans of DNA as measured from the vector-host genome junction to the shear site, are generated. Following sequencing, the number of spans for each unique integration can also be determined. The number of unique integration spans are not as susceptible to PCR biases as unique integration capture frequency.<sup>57, 58</sup> Using the spans for each unique integration, the percent contribution of each unique RIS was assessed for each mouse within a transplant group (Figure 5a-c) and then compiled for an overall comparison between vectors (Figure 5d). The magnitude of the integrations with the largest contribution to the total captured RIS were variable and highly dependent on the vector used to transduce the SRCs. These integrations can potentially impart a survival or growth advantage leading to clonal dominance. The control FVSGW and FVSGW-650cHS4-R transduced SRCs had similar clonal dominance. On average, approximately 75% of the observed spans were attributable to the top ten captured integrations from each mouse. A single clone making up more than 20% of the total population has been considered to be significant in the evaluation of clonal dominance.<sup>59</sup> One mouse with FVSGW transduced SRCs (B) had an individual clone contributing more than 20% of the total captured spans by week 27. Two mice transduced with FVSGW-650cHS4-R (B and E) also had dominant clones making up more than 20% of the total population of cells with vector integrations, though only at 18 weeks. FVSGW mouse B had a single integration with the highest level of clonal dominance (21.9%). The contributions of the top ten captured integrations in SRCs from FVSGW-A1-F transduced

mice were lower ( $p < 0.005$ ) than either FVSGW or FVSGW-650cHS4-R (Figure 5d). However we cannot rule out that the different MOIs of 6.5 (FVSGW), 10 (FVSGW-650cHS4-R) and 17 (FVSGW-A1-F) may have affected clonal dominance.

The top ten contributing integrations to each mouse were further assessed for their proximity to proto-oncogenes. Few integrations were within 100 kbp of proto-oncogene TSS. Of those integrations four were recovered at both the 18 and 27 week time points of FVSGW transduced SRCs while only one or two were highly captured at both time points from A1 or 650cHS4 insulated FVSGW respectively (Table 3). Integrations from the FVSGW transduced samples were on average closer to proto-oncogene TSS than integrations from the insulated samples. None of the top ten integrations were near proto-oncogenes previously attributed to genotoxic side effects in clinical trials.

We were further interested to evaluate integration sites relative to TSS taking into account the clonal dominance of individual RIS. Therefore, we re-evaluated the distribution of integrations within and near genes and proto-oncogenes using the number of spans identified for each unique RIS (Figure 4b, Table 4). This approach takes into account the relative contribution of individual clones, when determining the integration profile. For FVSGW, the highest retrieval of integrations was from upstream of TSSs and was greatest within 1 kbp at both 18 and 27 weeks. Both insulated FV vectors had a reduced percentage of integration retrievals within 50 kbp upstream of TSS ( $p < 0.001$ ), with the greatest percent of retrievals per kbp being within 2.5 kbp downstream of a TSS. A1 insulated FV had the lowest percentage of integrations retrieved within 50 kbp of a TSS ( $p < 0.001$ ). A1 also had the lowest percentage of integrations retrieved from within 50 kbp of a proto-oncogene TSS ( $p < 0.001$ ). Together this suggests that the A1 and 650cHS4 insulators impact clonal dominance differently than the uninsulated control, with more repopulating cells having integrations 3' of TSS, while the control has more integrations 5' of TSS.

We also evaluated RIS in the spleen. Spleens were collected from the mice and the DNA from the recovered cells processed by MGS-PCR. Similar to the bone marrow, the cells from the spleen showed an oligoclonal distribution of cells with integrated vector proviruses. FVSGW-A1-F transduced SRCs in the spleen were again highly polyclonal (Supplemental Figure S4). The top ten contributing integrations from the bone marrow of all vector transduced mice were present in the spleen regardless of the vector (data not shown).

## DISCUSSION

Retroviral vector mediated gene therapy has great potential as an effective and permanent therapy for HSC disorders as well as other acquired or inherited genetic diseases. Though potentially more efficacious than donor stem cell transplant,<sup>1</sup> severe vector mediated adverse side effects are of significant concern and limit widespread use of this therapy in the clinic. Recently, we described the development of an insulated FV vector with the potential to reduce vector mediated adverse side effects.<sup>19</sup> Here we describe the development of additional high titer insulated FV vectors with the recently identified A1 and A2 insulators from the human genome.<sup>50</sup> We then continued our investigation of vector safety by evaluating the effects of our newly developed insulated FV vectors on transplanted human



CD34<sup>+</sup> cells in the established NSG mouse model. Here we show that mice with A1 insulated FV vector transduced SRCs are polyclonal, potentially more so than 650cHS4 insulated FV vectors. We also show that insulators greatly affect the distribution of captured RIS within proximity to TSS and proto-oncogenes.

In order to be effective in the clinic, insulated FV vectors must be high titer and the insulator should be efficiently copied from the 3' LTR to the 5' LTR during reverse transcription. This results in a transgene cassette that is flanked by the insulator. The newly described A1 and A2 human insulators fulfilled these requirements. These insulators did not statistically reduce the titer of FV vectors and showed moderate insulating activity, decreasing promoter activity by about 35%. Insulated FV vector titer and insulator activity were not dependent on insulator orientation. In comparison, the previously described 650cHS4 insulator reduced titer by 3–5 fold and decreased promoter activity by 65% in the reverse orientation while reducing titer by 5–7 fold and decreasing promoter activity by 60% in the forward orientation.<sup>19</sup> The A1 and A2 insulators have a single CTCF binding site similar to the 650cHS4 and as expected, vector proviruses with the A1 and A2 insulators in both the 5' and 3' LTRs were consistently captured. This shows that the insulators are retained and effectively copied during reverse transcription and integration and should be present when used for clinical applications.

Previous reports of A1 and A2 showed that these insulators had more activity than a cHS4 insulator.<sup>50</sup> In that report, the insulators were not in the presence of a vector LTR and cHS4 was only evaluated in the forward orientation. When the activity of A1 and A2 were compared to a forward oriented 650cHS4 without the FV vector LTR, the A1 and A2 did have the greater activity, consistent with previous reports. However, the 650cHS4 is stronger in the reverse orientation<sup>19</sup> and has activity similar to the A1 and A2 insulators (Figure 1b). The activity of the 650cHS4 insulator further increases when in the FV vector LTR,<sup>19</sup> while the activity of the A1 and A2 insulators remains the same (Figure 1c). This highlights the importance of evaluating insulator activity within vector LTRs and in different orientations.

The A1 insulated FV vector fulfilled the criteria for a promising insulated vector. The insulating activity of A1 was significant and the insulated FV vector is higher titer than the previously described 650cHS4 insulated vector (Figure 1c–d). Using vectors with a strong promoter to maximize the potential genotoxic effects of an FV vector on the host genome, we showed that the A1 insulator promotes differences in the position of recovered integrations from in vitro cultured human CD34<sup>+</sup> cord blood cells (Figure 2a). Previously, the 650cHS4 insulated FV vector was shown to have a similar integration profile to the control uninsulated but decreased the number of integrations with 50 kbp sized hotspots.<sup>19</sup> In contrast, the presence of the A1 insulator appears to potentially promote a change in the integration profile causing integrations to occur even less frequently near TSS's than the uninsulated FV vector which already has reduced integrations near TSS's than gammaretroviral vectors. The increased frequency of gammaretroviral vector integrations near TSS's has been implicated in its genotoxicity<sup>17, 48, 60</sup>, therefore the reduction in integrations near TSS's imparted by the A1 insulator at transduction may improve safety. Integration sites at day five post-vector exposure are also found further away from proto-oncogene TSS and DNase hypersensitivity sites (Table 1). Future studies will be needed to

confirm this observation and to explore potential mechanisms. The process of FV integration site selection and integration is dictated by the pre-integration complex (PIC). This includes amino acids in the viral Gag protein which act as a DNA tether<sup>61</sup> as well as viral and host proteins which bind FV viral DNA prior to integration. Adding an insulator sequence to a retroviral vector is analogous to adding a protein binding site and thus could potentially recruit a host cell protein to the PIC. CTCF was previously shown to bind at A1 sites more often than cHS4.<sup>50</sup> Therefore CTCF could be binding the A1 insulated FV vector prior to integration and either redirecting where integration occurs or displacing other determinants of integration at a frequency detectable in this assay. Resolving the molecular mechanism of this change is outside the scope of the current manuscript. However, further evaluation of this potential insulator effect on integration profile will be of interest for the development of FV vectors and other gene therapy vectors.

The change in the integration profile potentially introduced by the A1 insulator was not evident following transplantation and successful engraftment in NSG mice (Figure 4a). However, fewer unique integrations were available from vector transduced SRCs than from in vitro cultures, as expected. The integration profiles based on unique integrations alone suggests that the A1 insulator may not promote safety compared to FV or 650cHS4 insulated FV vector. This is in contrast to previously published genotoxicity data comparing A1 insulated, cHS4 insulated, and wild type gammaretroviral vectors<sup>50</sup> as well as in contrast to the clonal contribution of captured integration sites presented in this paper. Therefore the integration profile was also assessed by magnitude of capture for different integration sites, which not only reestablishes a safer integration profile for A1 insulated FV vectors compared to wild type FV vectors but also shows a marked change to the integration profile imparted by insulators. (Figure 4b, Table 4). For both insulated vectors we found a drastic reduction in the total number of recovered integrations within 50 kbp upstream of the TSS (35%–40%,  $p < 0.001$  at week 27) relative to uninsulated FV vectors. Interestingly, insulators appear to promote the survival and expansion of cells with integrations within 2.5 kbp downstream of TSS, while uninsulated FV vectors promote expansion of cells with integrations within 2.5 kbp upstream of TSS. Overall A1 insulated proviruses were found with the least frequency within 50 kbp of TSSs and within genes. While the 650cHS4 insulated proviruses were recovered with the lowest frequency in immediate proximity to transcription start sites. 650cHS4 insulated proviruses were also found more frequently within genes, including proto-oncogenes. The difference in retrieval site distribution of uninsulated compared to insulated FV proviruses suggests that the insulator influences how vectors affect cell survival and expansion.

Assessing clonal dominance by evaluating the prevalence of each unique RIS is informative as to the safety of the different vectors. The A1 insulated FV vector appears to have reduced clonal expansion compared to both 650cHS4 insulated and control uninsulated FV vectors (Figure 5c,d). The magnitude of captured integrations here was assessed by the number of individual span lengths captured for each unique integration as opposed to the frequency of capture. Early methods of PCR amplification to capture integrated vector proviruses were restricted to relying solely on frequency of capture to assess clonal dominance. This was because RIS were either directly amplified from DNA by linear PCR, or from restriction enzyme digested DNA that would produce only one length of fragment for each vector

provirus. Recent adaptations of RIS capture approaches have utilized random shearing techniques (acoustic or mechanical shearing) to break the DNA into smaller sized fragments eliminating restriction enzyme site bias. In addition, this adds a unique length of DNA (span) from the RIS to the terminus of the sheared fragment. When clonal dominance occurs, several cells will contribute DNA with the same integration site but different spans. With shearing, not only is the frequency of capture obtained for each integration but also the number of different spans for each unique integration. Unlike frequency of capture which has been shown to have increased bias towards amplification of small fragments and gc rich fragments,<sup>62</sup> the total number of spans captured for each unique site is much less susceptible to these biases.<sup>57</sup>

The 650cHS4 insulator did not reduce clonal dominance compared to control FV. The most prevalent unique integration was retrieved from a mouse transplanted with FVSGW transduced human CD34<sup>+</sup> cells. This integration is less than 25 kbp from the proto-oncogene C-X-C motif chemokine ligand 1 (*CXCL1*). Also known as the GRO1 oncogene, *CXCL1* is a secreted protein involved in neutrophil chemotaxis. It is traditionally expressed on macrophages, neutrophils, and epithelial cells and is highly secreted by melanoma cells. Though not associated with leukomogenesis, it is part of a paracrine loop which imparts cancer chemoresistance.<sup>63</sup> Upregulation of this gene could give a selective growth advantage in the bone marrow without disrupting hematopoiesis though it could present a problem for the treatment of a potential future non-gene therapy related cancers. It is important to point out that in our study we used a SFFV promoter in order to promote clonal expansion and stress the ability of the insulator to protect from clonal dominance. Use of a less genotoxic promoter such as the phosphoglycerate kinase promoter (PGK) or elongation factor 1 $\alpha$  promoter (EF1 $\alpha$ ) should result in less clonal expansion and captured integrations near proto-oncogenes.

The A1 insulator did reduce dominance, but due to differences in post dialyztion vector recovery efficiencies, the A1 insulated FV vector transduced SRCs were exposed to a higher MOI. This resulted in a higher transduction efficiency of the A1 transduced cells and could increase the polyclonality of engrafted cells. Recently our laboratory has published a study comparing the polyclonality of lentiviral vector and a similar WT FV vector in transduced bone marrow SRCs.<sup>20</sup> In this study the percent transduction of CD34<sup>+</sup> cells prior to transplantation were much higher than in this study (50.1%) and the post transplantation EGFP in circulating SRCs was more similar at 19 weeks post-transplant. When the clonal distribution for these mice is compared to the current FVSGW-A1-F RIS data, we find that mice with A1 insulated FV vector transduced SRCs are still more polyclonal (~17% reduction to the prevalence of the top ten clones). At the current n this value does not quite reach statistical significance (p=0.088) (Supplemental Figure S5), however this data suggests A1 is very promising as an element that may increase the safety of retroviral vector gene therapy and is deserving of further investigation.

To our knowledge, this is the first report of RIS data from insulated retroviral vector exposed SRCs and is consistent with the genotoxicity studies done previously comparing A1 to cHS4.<sup>50</sup> Though relatively safe in in vitro assays, under the selective pressure of the xenotransplantation SRC model, the population of bone marrow cells from mice

transplanted with FVSGW-650cHS4-R transduced CD34<sup>+</sup> cells appear to be less polyclonal than the bone marrow from mice transplanted with FVSGW-A1-F transduced CD34<sup>+</sup> cells, although transduction frequency was 1.7 fold higher than the 650cHS4. We hypothesize that the 650cHS4 insulator is less effective at reducing selective growth advantages than the A1 insulator. However, the fact that both the A1 and 650cHS4 insulated vectors led to similarly different capture profiles than the control FV vector near TSS suggests a growth advantage may occur by a different mechanism for these two insulators. It has been shown that insulated vectors can affect the expression of tumor suppressor genes which shorten the life span of tumor prone mice in a genotoxicity model for lentiviral vectors.<sup>13</sup> The more moderate activity of the A1 insulator may have reduced negative effects caused by insulators while simultaneously maintaining enough effect on enhancers to reduce the genotoxicity seen from uninsulated vectors.

Our data further supports the use of SRCs to evaluate clonal expansion as an evaluation of vector safety and to further our understanding of how vector design may contribute to safety. Previously vector safety has been primarily evaluated in primary murine bone marrow in vitro or utilizing the 32D genotoxicity assay.<sup>14, 34, 64</sup> Immortalization of primary murine bone marrow has been used successfully to evaluate the genotoxicity of gammaretroviral vectors compared to lentiviral vectors.<sup>14, 64</sup> The 32D assay has been successfully utilized to establish differences in the genotoxicity of insulated and uninsulated gammaretroviral vectors.<sup>34</sup> However, this assay failed to identify any differences in safety between FV or insulated FV vectors.<sup>19</sup> More recently tumor prone mouse models, such as the *CDNK2A* knockout mouse, have been used to compare the safety of both insulated and uninsulated retroviral vectors.<sup>13, 65</sup> This model has shown significant differences in the survival of mice transplanted with vector transduced murine bone marrow cells, reflecting the safety of retroviral vectors when in vitro models have failed. However, this model still utilizes murine cells instead of the final intended target of HSC gene therapy, human CD34<sup>+</sup> cells. Evaluating clonal expansion in human cord blood CD34<sup>+</sup> repopulating cells may identify genotoxicity that cannot be evaluated in mouse cells.

In conclusion, we have developed a promising insulated FV vector for HSC gene therapy that contains the A1 insulator from chromosome 1 of the human genome.<sup>50</sup> This vector does not reduce FV vector titer, has insulating activity, and is maintained during vector production and integration. In a murine xenotransplantation model, this insulator resulted in a polyclonal population of transduced human CD34<sup>+</sup> cells. We have also shown that the retrieved RIS from transduced CD34<sup>+</sup> cells have a potentially safer integration profile than uninsulated FV. Results from a previous study comparing the clonality of cells transduced with uninsulated FVs to lentiviral vectors strongly suggest that FV vectors are potentially safer for HSC gene therapy.<sup>20</sup> Our data suggests that the A1 insulator further improves the safety of FV vectors. When combined with a clinically relevant promoter, such as EF1 $\alpha$  or PGK, A1 insulated FV vectors may be highly effective and safe. Promising preclinical data from future studies using insulated FV vectors with a clinically relevant promoter in SRCs and the dog large animal model will be important for translation of insulated FV vectors to the clinic. Our data suggests that an A1 insulated FV is an extremely promising vector for HSC gene therapy and supports further evaluation in pre-clinical and clinical therapeutic trials.

## MATERIALS AND METHODS

### Cell culture

HEK293T and HT1080 fibroblasts were cultured in Hyclone high glucose DMEM (Thermo Scientific SH30022.01, Waltham, MA) supplemented with 10% fetal bovine serum (FBS) (Atlanta Biologicals S11550, Lawrenceville, GA) and 50 U/mL penicillin and streptomycin (Lonza 17-602E, Walkersville, MD). Cell lines were maintained at 37°C and 5% CO<sub>2</sub>.

### Plasmids and plasmid construction

FVSGW and FVSGW-650cHS4-R were previously described.<sup>19</sup> The FVSGW-A1 and A2 vectors were made by cloning synthesized *Nsi*I restriction site flanked A1 and A2 insulators into FVSGW using standard cloning techniques. FVSGWKO-A1 and FVSGWKO-A2 vectors were developed by cloning a *Sal*I restriction site flanked R6Kgamma bacterial origin of replication and kanamycin resistance cassette into the *Sal*I restriction site within FVSGW-A1 and FVSGW-A2. Insulators were synthesized by GenScript (Piscataway, NJ).

### Vector production and titer

FV vector production and titer were performed as previously described.<sup>18, 19, 66</sup> Briefly, HEK293T cell were plated on poly-L-lysine coated plates and transfected with vector and vector packaging helper plasmids with polyethylenimine (PEI). Final vector preparations were concentrated by centrifugation and stored in 1:100 the original volume of serum free IMDM and 5% DMSO. Functional titer of all vectors were determined by flow cytometric analysis of EGFP expressing HT1080 fibroblasts following transduction.

### Enhancer blocking activity assay

Enhancer blocking activity test plasmids and assay were performed as previously described.<sup>19</sup> The mean mCherry fluorescence intensity (MFI) was determined for the EGFP positive cells transfected with control (no insert), LTR, insulator, or insulated LTR containing enhancer blocking activity assay plasmid. To compensate for differences in transfection efficiency, the mCherry MFI was divided by the EGFP MFI to normalize the mCherry expression. The percent of control (no insert) expression was then determined. Control expression normalized to 100%.

### Shuttle vector rescue for insulator fidelity

Shuttle vector rescue of DNA extracted from transduced HT1080 fibroblasts was performed as previously described.<sup>19</sup> Sequencing was performed (Genewiz, South Plainfield, NJ) using primers 5'-*TATGCCTCCCGCTATGCTCG*-3' and 5'-*CCTGTGGAACACCTACATCTG*-3' for the 5' and 3' LTRs respectively.

### Transduction and in vitro culture of human CD34<sup>+</sup> cord blood cells

Cryopreserved male human CD34<sup>+</sup> cord blood cells were thawed and pooled from three male donors (Cat # 70008.5, STEMCELL Technologies, Vancouver, BC, Canada) and maintained between 5×10<sup>5</sup> and 1×10<sup>6</sup> cells/ mL. Prestimulation and transductions were conducted as previously described.<sup>18</sup> Briefly, human CD34<sup>+</sup> cells were thawed as per the

manufacturer instructions and pre-stimulated at 37°C for 18 hrs in IMDM with 10% heat inactivated FBS, 5000U penicillian/streptomycin, and 100 ng/ mL of the recombinant human cytokines IL-3, IL-6, SCF, TPO, Flt-3, and G-CSF. Cells were then counted and transferred to non-TC treated plates coated with 2 ug/ cm<sup>2</sup> RetroNectin (Cat # T100A, Takara Bio, Otsu, Shiga, Japan) as per the manufacturer instructions. Vector preparations were dialyzed (UFC505024, Fisher Scientific, Waltham, MA, USA) to remove DMSO and then added to cells at a target multiplicity of infection (MOI) of 10. Following a post dialyzation titer, the MOI's were back calculated to 6.5, 10, and 17 for FVSGW, FVSGW-650cHS4-R, and FVSGW-A1-F respectively. The day following vector exposure, cells were harvested and prepared for transplantation. Remaining cells were retained in culture for up to ten days and the EGFP expression and vector integration sites (RIS) determined at day five and day ten post vector exposure.

### Xenotransplantation

Animal protocols have been approved by the Washington State University Institutional Animal Care and Use Committee. NSG mice (NOD.Cg-Prkdc<sup>scid</sup>Il2rg<sup>tm1Wjl</sup>/SzJ, Cat # 005557, The Jackson Laboratory, Bar Harbor, ME, USA) were housed in sterile microisolator cages and given water and food ad libitum. Three days prior to CD34<sup>+</sup> cell transplantation, mice were given tetracycline treated water and maintained on antibiotic water for four weeks. At 48 and 24 hours prior to transplantation, four week old NSG mice were given a 25 mg/ kg of body weight busulfan dose in a 1:3 ratio of DMSO and RPMI intraperitoneally. At the time of transplant transduced human CD34<sup>+</sup> cord blood cells were harvested and suspended at 5×10<sup>5</sup> cells/ mL in phosphate buffered saline (PBS). 1×10<sup>5</sup> cells were transplanted into each mouse via the tail vein. Every three weeks starting at week six, 100–200 µL of peripheral blood was extracted from the right saphenous vein of each mouse to evaluate engraftment by flow cytometric analysis. At 18 weeks post-transplant, mice were sedated with isoflurane and up to 3 µL bone marrow extracted from either the right or left femur. Mice were euthanized 27 weeks post transplantation<sup>67</sup> and bone marrow from the right and left legs, blood, and spleens collected.

### Flow cytometric analysis of murine blood and bone marrow

50 µL peripheral blood or ~5×10<sup>5</sup> bone marrow cells in PBS with 10% FBS were blocked with anti-mouse CD16/CD32 (cat # 101302, Biolegend, San Diego, CA, USA) and then stained with fluorophore conjugated antibodies. Following staining, red blood cells were lysed with RBC lysis buffer (cat # sc-296258, Santa Cruz Biotechnology, Dallas, TX, USA) for 10 min and washed twice with 10% FBS in PBS. Peripheral blood samples underwent a second 5 min RBC lysis prior to washing. Samples were acquired on a BD Accuri C6 or Beckman coulter Gallios flow cytometer and analyzed using BD Accuri C sampler software or FlowJo. Cells were stained with anti-human CD34 PE (cat # 343606, Biolegend), anti-human CD11b PE (cat # 555388, BD Biosciences, San Jose, CA, USA), anti-human CD3 PE/Dazzle™ 594 (cat # 300450, Biolegend), anti-mouse CD45 PerCP-Cy5.5 (cat # 103132 Biolegend), anti-mouse CD45 PerCP (cat # 557235, BD), anti-human CD19 PE-Cy7 (cat # 302216, Biolegend), anti-human CD45 APC (cat # 555485, BD Bioscience or cat # 304012, Biolegend). Analysis based 10 000 bone marrow and 3 000 blood cells from the live cell gate.

## Modified genomic sequencing (MGS)-PCR

DNA was extracted from bone marrow samples (Gentra puregene blood kit, cat # 158445, Qiagen,) and spleens (Gentra puregene cell and tissue kit). 3 µg of genomic DNA from each mouse was modified genomic sequencing (MGS)-PCR processed as previously described<sup>19, 58, 68</sup> and sequenced on an Illumina MiSeq (Genomic Sequencing and Analysis Facility, University of Texas-Austin, Austin, TX). Sequences were paired with Paired-End read mergeR (PEAR) software<sup>69</sup> and processed with the Vector Integration Site Analysis (VISA) server as done previously.<sup>19, 70</sup> Sample overlap is common<sup>68, 71–73</sup> and was resolved by comparing the span counts for each unique RIS between a VISA compiled data set and the data sets for each individual mouse at each time point. Unique RIS were attributed to the mice with a span count identical to the span count in the combined data set. When the span count in the combined data set was greater than the span count of any individual mouse, the RIS was attributed to the mouse which contained 80% or more of the total RIS and had at least three times as many spans as seen in another mouse. Overlapping RIS which did not meet the above criteria or with 10 span counts or less in the combined data set were not resolved and remain as unique RIS for each individual mouse.

## Statistical analysis

Statistical significance was evaluated by ANOVA and validated by two-tailed student T-test for procedures performed in triplicate or more.  $\chi^2$  analysis was used to evaluate statistically significant differences of MGS-PCR retroviral vector integration site data. p value less than 0.05 was considered statistically significant.

## Supplementary Material

Refer to Web version on PubMed Central for supplementary material.

## Acknowledgments

This work was supported by NIH grants AI097100 and AI102672 (GDT). The authors would also like to acknowledge the WSU Spokane flow cytometry core.

## References

1. Touzot F, Moshous D, Creidy R, Neven B, Frange P, Cros G, et al. Faster T-cell development following gene therapy compared with haploidentical HSCT in the treatment of SCID-X1. *Blood*. 2015; 125(23):3563–9. [PubMed: 25869287]
2. Kiem HP, Sellers S, Thomasson B, Morris JC, Tisdale JF, Horn PA, et al. Long-term clinical and molecular follow-up of large animals receiving retrovirally transduced stem and progenitor cells: no progression to clonal hematopoiesis or leukemia. *Mol Ther*. 2004; 9(3):389–95. [PubMed: 15006605]
3. Carbonaro DA, Zhang L, Jin X, Montiel-Equihua C, Geiger S, Carmo M, et al. Preclinical demonstration of lentiviral vector-mediated correction of immunological and metabolic abnormalities in models of adenosine deaminase deficiency. *Mol Ther*. 2014; 22(3):607–22. [PubMed: 24256635]
4. Bordignon C, Notarangelo LD, Nobili N, Ferrari G, Casorati G, Panina P, et al. Gene therapy in peripheral blood lymphocytes and bone marrow for ADA- immunodeficient patients. *Science*. 1995; 270(5235):470–5. [PubMed: 7570000]

5. Hacein-Bey-Abina S, Le Deist F, Carlier F, Bouneaud C, Hue C, De Villartay JP, et al. Sustained correction of X-linked severe combined immunodeficiency by ex vivo gene therapy. *N Engl J Med.* 2002; 346(16):1185–93. [PubMed: 11961146]
6. Cavazzana-Calvo M, Payen E, Negre O, Wang G, Hehir K, Fusil F, et al. Transfusion independence and HMG2 activation after gene therapy of human beta-thalassaemia. *Nature.* 2010; 467(7313): 318–22. [PubMed: 20844535]
7. Aiuti A, Biasco L, Scaramuzza S, Ferrua F, Cicalese MP, Baricordi C, et al. Lentiviral hematopoietic stem cell gene therapy in patients with Wiskott-Aldrich syndrome. *Science.* 2013; 341(6148): 1233151. [PubMed: 23845947]
8. Hacein-Bey-Abina S, Garrigue A, Wang GP, Soulier J, Lim A, Morillon E, et al. Insertional oncogenesis in 4 patients after retrovirus-mediated gene therapy of SCID-X1. *The Journal of clinical investigation.* 2008; 118(9):3132–42. [PubMed: 18688285]
9. Stein S, Ott MG, Schultze-Strasser S, Jauch A, Burwinkel B, Kinner A, et al. Genomic instability and myelodysplasia with monosomy 7 consequent to EVI1 activation after gene therapy for chronic granulomatous disease. *Nature medicine.* 2010; 16(2):198–204.
10. Braun CJ, Boztug K, Paruzynski A, Witzel M, Schwarzer A, Rothe M, et al. Gene therapy for Wiskott-Aldrich syndrome--long-term efficacy and genotoxicity. *Science translational medicine.* 2014; 6(227):227–233.
11. Trobridge GD. Genotoxicity of retroviral hematopoietic stem cell gene therapy. *Expert Opin Biol Ther.* 2011; 11(5):581–593. [PubMed: 21375467]
12. Hargrove PW, Kepes S, Hanawa H, Obenauer JC, Pei D, Cheng C, et al. Globin lentiviral vector insertions can perturb the expression of endogenous genes in beta-thalassemic hematopoietic cells. *Mol Ther.* 2008; 16(3):525–33.
13. Cesana D, Ranzani M, Volpin M, Bartholomae C, Duros C, Artus A, et al. Uncovering and dissecting the genotoxicity of self-inactivating lentiviral vectors in vivo. *Mol Ther.* 2014; 22(4): 774–85. [PubMed: 24441399]
14. Arumugam PI, Higashimoto T, Urbinati F, Modlich U, Nestheide S, Xia P, et al. Genotoxic potential of lineage-specific lentivirus vectors carrying the beta-globin locus control region. *Mol Ther.* 2009; 17(11):1929–37.
15. Ott MG, Schmidt M, Schwarzwaelder K, Stein S, Siler U, Koehl U, et al. Correction of X-linked chronic granulomatous disease by gene therapy, augmented by insertional activation of MDS1-EVI1, PRDM16 or SETBP1. *Nature medicine.* 2006; 12(4):401–9.
16. Siler U, Paruzynski A, Holtgreve-Grez H, Kuzmenko E, Koehl U, Renner ED, et al. Successful Combination of Sequential Gene Therapy and Rescue Allo-HSCT in Two Children with X-CGD - Importance of Timing. *Current gene therapy.* 2015; 15(4):416–27. [PubMed: 25981636]
17. Trobridge GD, Miller DG, Jacobs MA, Allen JM, Kiem HP, Kaul R, et al. Foamy virus vector integration sites in normal human cells. *Proceedings of the National Academy of Sciences of the United States of America.* 2006; 103(5):1498–503. [PubMed: 16428288]
18. Olszko ME, Adair JE, Linde I, Rae DT, Trobridge P, Hocum JD, et al. Foamy viral vector integration sites in SCID-repopulating cells after MGMTP140K-mediated in vivo selection. *Gene therapy.* 2015; 22(7):591–5. [PubMed: 25786870]
19. Browning DL, Collins CP, Hocum JD, Leap D, Rae DT, Trobridge GD. Insulated Foamy Viral Vectors. *Hum Gene Ther.* 2016; 27(3):255–66. [PubMed: 26715244]
20. Everson EM, Olszko ME, Leap DJ, Hocum JD, Trobridge GD. A direct comparison of foamy and lentiviral vector genotoxicity in SCID-repopulating cells shows foamy vectors are less prone to clonal dominance. *Mol Ther Methods Clin Dev.* 2016; 3(16048)
21. Trobridge G. Improved Foamy Virus Vectors with Minimal Viral Sequences. *Molecular Therapy.* 2002; 6(3):321–328. [PubMed: 12231167]
22. Bokhoven M, Stephen SL, Knight S, Gevers EF, Robinson IC, Takeuchi Y, et al. Insertional gene activation by lentiviral and gammaretroviral vectors. *Journal of virology.* 2009; 83(1):283–94. [PubMed: 18945765]
23. Nowrouzi A, Dittrich M, Klanke C, Heinkelein M, Rammling M, Dandekar T, et al. Genome-wide mapping of foamy virus vector integrations into a human cell line. *The Journal of general virology.* 2006; 87(Pt 5):1339–47. [PubMed: 16603537]



24. Nasimuzzaman M, Kim YS, Wang YD, Persons DA. High-titer foamy virus vector transduction and integration sites of human CD34(+) cell-derived SCID-repopulating cells. *Mol Ther Methods Clin Dev.* 2014; 1:14020. [PubMed: 26015964]
25. Hendrie PC, Huo Y, Stolitenko RB, Russell DW. A rapid and quantitative assay for measuring neighboring gene activation by vector proviruses. *Mol Ther.* 2008; 16(3):534–40. [PubMed: 18209733]
26. Josephson NC, Trobridge G, Russell DW. Transduction of long-term and mobilized peripheral blood-derived NOD/SCID repopulating cells by foamy virus vectors. *Hum Gene Ther.* 2004; 15(1):87–92. [PubMed: 14965380]
27. Trobridge GD, Allen J, Peterson L, Ironside C, Russell DW, Kiem HP. Foamy and lentiviral vectors transduce canine long-term repopulating cells at similar efficiency. *Hum Gene Ther.* 2009; 20(5): 519–23. [PubMed: 19199822]
28. Miccio A, Poletti V, Tiboni F, Rossi C, Antonelli A, Mavilio F, et al. The GATA1-HS2 enhancer allows persistent and position-independent expression of a beta-globin transgene. *PloS one.* 2011; 6(12):e27955. [PubMed: 22164220]
29. Negre O, Eggimann AV, Beuzard Y, Ribeil JA, Bourget P, Borwornpinyo S, et al. Gene Therapy of the  $\beta$ -Hemoglobinopathies by Lentiviral Transfer of the  $\beta$ (A(T87Q))-Globin Gene. *Hum Gene Ther.* 2016; 27(2):148–65. [PubMed: 26886832]
30. Bauer TR Jr, Allen JM, Hai M, Tuschong LM, Khan IF, Olson EM, et al. Successful treatment of canine leukocyte adhesion deficiency by foamy virus vectors. *Nature medicine.* 2008; 14(1):93–7.
31. Bauer TR Jr, Olson EM, Huo Y, Tuschong LM, Allen JM, Li Y, et al. Treatment of canine leukocyte adhesion deficiency by foamy virus vectors expressing CD18 from a PGK promoter. *Gene therapy.* 2011; 18(6):553–9. [PubMed: 21228879]
32. Hunter MJ, Zhao H, Tuschong LM, Bauer TR Jr, Burkholder TH, Persons DA, et al. Gene therapy for canine leukocyte adhesion deficiency with lentiviral vectors using the murine stem cell virus and human phosphoglycerate kinase promoters. *Hum Gene Ther.* 2011; 22(6):689–96. [PubMed: 21275758]
33. Booth C, Gaspar HB, Thrasher AJ. Treating Immunodeficiency through HSC Gene Therapy. *Trends Mol Med.* 2016; 22(4):317–27. [PubMed: 26993219]
34. Li CL, Xiong D, Stamatoyannopoulos G, Emery DW. Genomic and functional assays demonstrate reduced gammaretroviral vector genotoxicity associated with use of the cHS4 chromatin insulator. *Mol Ther.* 2009; 17(4):716–24. [PubMed: 19240697]
35. Ramezani A, Hawley TS, Hawley RG. Performance- and safety-enhanced lentiviral vectors containing the human interferon-beta scaffold attachment region and the chicken beta-globin insulator. *Blood.* 2003; 101(12):4717–24. [PubMed: 12586614]
36. Felsenfeld G. Chromatin structure and the expression of globin-encoding genes. *Gene.* 1993; 135(1–2):119–24. [PubMed: 8276248]
37. Chung JH, Whiteley M, Felsenfeld G. A 5' element of the chicken beta-globin domain serves as an insulator in human erythroid cells and protects against position effect in *Drosophila*. *Cell.* 1993; 74(3):505–14. [PubMed: 8348617]
38. Bell AC, West AG, Felsenfeld G. Insulators and boundaries: versatile regulatory elements in the eukaryotic genome. *Science.* 2001; 291(5503):447–50. [PubMed: 11228144]
39. Burgess-Beusse B, Farrell C, Gaszner M, Litt M, Mutskov V, Recillas-Targa F, et al. The insulation of genes from external enhancers and silencing chromatin. *Proceedings of the National Academy of Sciences of the United States of America.* 2002; 99(Suppl 4):16433–7. [PubMed: 12154228]
40. West AG, Gaszner M, Felsenfeld G. Insulators: many functions, many mechanisms. *Genes & development.* 2002; 16(3):271–88. [PubMed: 11825869]
41. Wallace JA, Felsenfeld G. We gather together: insulators and genome organization. *Current opinion in genetics & development.* 2007; 17(5):400–7. [PubMed: 17913488]
42. Sun FL, Elgin SC. Putting boundaries on silence. *Cell.* 1999; 99(5):459–62. [PubMed: 10589674]
43. Splinter E, Heath H, Kooren J, Palstra RJ, Klous P, Grosveld F, et al. CTCF mediates long-range chromatin looping and local histone modification in the beta-globin locus. *Genes & development.* 2006; 20(17):2349–54. [PubMed: 16951251]

44. Emery DW. The use of chromatin insulators to improve the expression and safety of integrating gene transfer vectors. *Hum Gene Ther.* 2011; 22(6):761–74. [PubMed: 21247248]
45. Neff T, Shotkoski F, Stamatoyannopoulos G. Stem cell gene therapy, position effects and chromatin insulators. *Stem cells.* 1997; 15(Suppl 1):265–71. [PubMed: 9368350]
46. Arumugam PI, Urbinati F, Velu CS, Higashimoto T, Grimes HL, Malik P. The 3' region of the chicken hypersensitive site-4 insulator has properties similar to its core and is required for full insulator activity. *PloS one.* 2009; 4(9):e6995. [PubMed: 19746166]
47. Gaussin A, Modlich U, Bauche C, Niederlander NJ, Schambach A, Duros C, et al. CTF/NF1 transcription factors act as potent genetic insulators for integrating gene transfer vectors. *Gene therapy.* 2012; 19(1):15–24. [PubMed: 21562592]
48. Montini E, Cesana D, Schmidt M, Sanvito F, Bartholomae CC, Ranzani M, et al. The genotoxic potential of retroviral vectors is strongly modulated by vector design and integration site selection in a mouse model of HSC gene therapy. *The Journal of clinical investigation.* 2009; 119(4):964–75. [PubMed: 19307726]
49. Zychlinski D, Schambach A, Modlich U, Maetzig T, Meyer J, Grassman E, et al. Physiological promoters reduce the genotoxic risk of integrating gene vectors. *Mol Ther.* 2008; 16(4):718–25. [PubMed: 18334985]
50. Liu, M., Maurano, MT., Wang, H., Qi, H., Song, CZ., Navas, PA., et al. *Nat Biotechnol.* Vol. 33. United States: 2015. Genomic discovery of potent chromatin insulators for human gene therapy; p. 198-203.
51. Chen H, Tian Y, Shu W, Bo X, Wang S. Comprehensive identification and annotation of cell type-specific and ubiquitous CTCF-binding sites in the human genome. *PloS one.* 2012; 7(7):e41374. [PubMed: 22829947]
52. Follows GA, Ferreira R, Janes ME, Spensberger D, Cambuli F, Chaney AF, et al. Mapping and functional characterisation of a CTCF-dependent insulator element at the 3' border of the murine *Scl* transcriptional domain. *PloS one.* 2012; 7(3):e31484. [PubMed: 22396734]
53. Kim TH, Abdullaev ZK, Smith AD, Ching KA, Loukinov DI, Green RD, et al. Analysis of the vertebrate insulator protein CTCF-binding sites in the human genome. *Cell.* 2007; 128(6):1231–45. [PubMed: 17382889]
54. Xie X, Mikkelsen TS, Gnirke A, Lindblad-Toh K, Kellis M, Lander ES. Systematic discovery of regulatory motifs in conserved regions of the human genome, including thousands of CTCF insulator sites. *Proceedings of the National Academy of Sciences of the United States of America.* 2007; 104(17):7145–50. [PubMed: 17442748]
55. Weber EL, Cannon PM. Promoter choice for retroviral vectors: transcriptional strength versus trans-activation potential. *Hum Gene Ther.* 2007; 18(9):849–60. [PubMed: 17767401]
56. Cattoglio, C., Facchini, G., Sartori, D., Antonelli, A., Miccio, A., Cassani, B., et al. *Blood.* Vol. 110. United States: 2007. Hot spots of retroviral integration in human CD34+ hematopoietic cells. In; p. 1770-8.
57. Zhou S, Bonner MA, Wang YD, Rapp S, De Ravin SS, Malech HL, et al. Quantitative shearing linear amplification polymerase chain reaction: an improved method for quantifying lentiviral vector insertion sites in transplanted hematopoietic cell systems. *Hum Gene Ther Methods.* 2015; 26(1):4–12. [PubMed: 25545666]
58. Rae DT, Collins CP, Hocum JD, Browning DL, Trobridge GD. Modified Genomic Sequencing PCR Using the MiSeq Platform to Identify Retroviral Integration Sites. *Hum Gene Ther Methods.* 2015
59. Corrigan-Curay, J., Cohen-Haguenauer, O., O'Reilly, M., Ross, SR., Fan, H., Rosenberg, N., et al. *Mol Ther.* Vol. 20. United States: 2012. Challenges in vector and trial design using retroviral vectors for long-term gene correction in hematopoietic stem cell gene therapy; p. 1084-94.
60. Liu M, Li CL, Stamatoyannopoulos G, Dorschner MO, Humbert R, Stamatoyannopoulos JA, et al. Gammaretroviral vector integration occurs overwhelmingly within and near DNase hypersensitive sites. *Hum Gene Ther.* 2012; 23(2):231–7. [PubMed: 21981728]
61. Tobaly-Tapiero J, Bittoun P, Lehmann-Che J, Delelis O, Giron ML, de The H, et al. Chromatin tethering of incoming foamy virus by the structural Gag protein. *Traffic (Copenhagen, Denmark).* 2008; 9(10):1717–27.

62. Dabney J, Meyer M. Length and GC-biases during sequencing library amplification: a comparison of various polymerase-buffer systems with ancient and modern DNA sequencing libraries. *Biotechniques*. 2012; 52(2):87–94. [PubMed: 22313406]
63. Acharyya S, Oskarsson T, Vanharanta S, Malladi S, Kim J, Morris PG, et al. A CXCL1 paracrine network links cancer chemoresistance and metastasis. *Cell*. 2012; 150(1):165–78. [PubMed: 22770218]
64. Ramezani A, Hawley TS, Hawley RG. Combinatorial incorporation of enhancer-blocking components of the chicken beta-globin 5'HS4 and human T-cell receptor alpha/delta BEAD-1 insulators in self-inactivating retroviral vectors reduces their genotoxic potential. *Stem cells*. 2008; 26(12):3257–66. [PubMed: 18787211]
65. Montini E, Cesana D. Genotoxicity assay for gene therapy vectors in tumor prone *Cdkn2a(-)/(-)* mice. *Methods in enzymology*. 2012; 507:171–85. [PubMed: 22365774]
66. Kiem HP, Wu RA, Sun G, von Laer D, Rossi JJ, Trobridge GD. Foamy combinatorial anti-HIV vectors with MGMTP140K potently inhibit HIV-1 and SHIV replication and mediate selection in vivo. *Gene therapy*. 2010; 17(1):37–49. [PubMed: 19741733]
67. Cheung AM, Nguyen LV, Carles A, Beer P, Miller PH, Knapp DJ, et al. Analysis of the clonal growth and differentiation dynamics of primitive barcoded human cord blood cells in NSG mice. *Blood*. 2013; 122(18):3129–37. [PubMed: 24030380]
68. Beard BC, Adair JE, Trobridge GD, Kiem HP. High-throughput genomic mapping of vector integration sites in gene therapy studies. *Methods Mol Biol*. 2014; 1185:321–44. [PubMed: 25062639]
69. Zhang, J., Kobert, K., Flouri, T., Stamatakis, A. *Bioinformatics*. Vol. 30. England: 2014. PEAR: a fast and accurate Illumina Paired- End reAd mergeR; p. 614-20.
70. Hocum JD, Battrell LR, Maynard R, Adair JE, Beard BC, Rawlings DJ, et al. VISA - Vector Integration Site Analysis server: a web-based server to rapidly identify retroviral integration sites from next-generation sequencing. *BMC bioinformatics*. 2015; 16:212. [PubMed: 26150117]
71. Brugman MH, Suerth JD, Rothe M, Suerbaum S, Schambach A, Modlich U, et al. Evaluating a ligation-mediated PCR and pyrosequencing method for the detection of clonal contribution in polyclonal retrovirally transduced samples. *Hum Gene Ther Methods*. 2013; 24(2):68–79. [PubMed: 23384086]
72. Gabriel R, Kutschera I, Bartholomae CC, von Kalle C, Schmidt M. Linear amplification mediated PCR--localization of genetic elements and characterization of unknown flanking DNA. *J Vis Exp*. 2014; (88):e51543. [PubMed: 24998871]
73. Lu R, Neff NF, Quake SR, Weissman IL. Tracking single hematopoietic stem cells in vivo using high-throughput sequencing in conjunction with viral genetic barcoding. *Nat Biotechnol*. 2011; 29(10):928–33. [PubMed: 21964413]

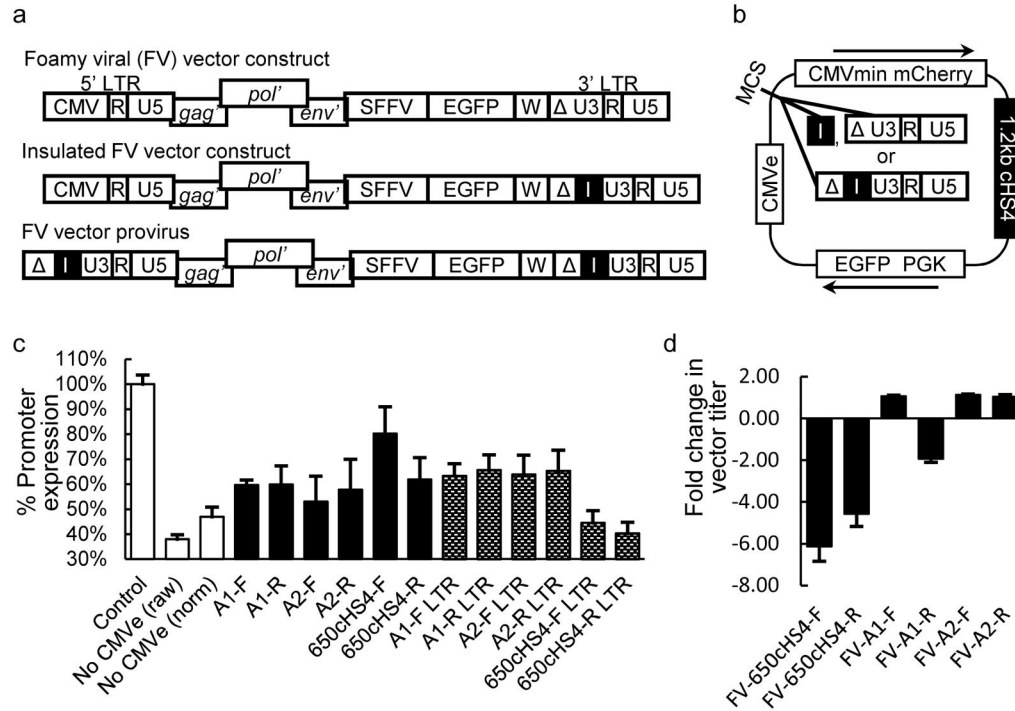


**Figure 1.** Efficacy of A1 and A2 insulators in foamy viral (FV) vectors. (a) Insulated FV vector construction. Insulators (black box labeled I) were placed in the 3' long terminal repeat (LTR) U3. During reverse transcription, the 3'LTR, including insulator, is copied to the 5' LTR. Integration competent FV vector genome is flanked by insulator containing LTRs. FV vector contains portions (\*) of the FV *gag*, *pol*, and *env* sequences necessary for vector genome packaging and integration. The FV vector LTR in plasmid form contains a CMV fusion LTR for the purposes of vector production and the woodchuck hepatitis virus posttranscriptional regulatory element (W) for enhanced gene expression. (b) Enhancer blocking activity test plasmid. The CMV enhancer (CMVe) and CMV minimal promoter (CMVmin) are separated by 400 bps and a multiple cloning site (MCS) for the addition of elements to be tested for enhancer blocking activity. (c) Activity of insulators and insulated FV LTRs. Insulators were assessed alone and within the foamy virus long terminal repeat (LTR) for activity in the enhancer-blocking activity assay. The percent of remaining promoter activity as based on mCherry expression following addition of the indicated insulators is shown. A control plasmid without an insulator (control) as well as a control plasmid without an enhancer and insulator (no CMVe) were assessed to determine the upper and lower limits of expression. Both the non-normalized mCherry (raw) and EGFP normalized mCherry (norm) are shown. (d) Effect of insulators on FV vector titer. The fold change as compared to uninsulated FV vectors is shown. Data for 650cHS4 and 650cHS4 insulated vectors reproduced from Browning, et al. (2016) Human Gene Therapy, 27:255–266. Error bars represent standard deviation (SD).

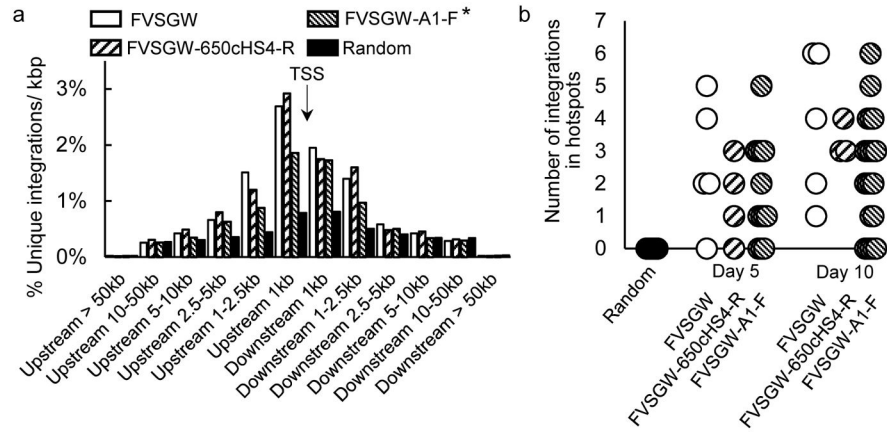


**Figure 2.** Retroviral vector integration site (RIS) analysis of insulated and uninsulated vector exposed human CD34<sup>+</sup> cells. (a) The positions of unique FV vector integrations in transduced human cord blood cells relative to RefSeq gene transcription start sites five days post vector exposure. FVSGW, n= 1747; FVSGW-650cHS4-R, n= 1200; FVSGW-A1-F, n= 4109. \* is p<0.001 (b) CD34<sup>+</sup> stem cells from cord blood were transduced with insulated or uninsulated FV vectors and cultured in vitro for five or ten days prior to genomic DNA extraction for modified genomic sequencing- polymerase chain reaction (MGS-PCR). Captured integrations were ordered by position in the genome and the distances between the nearest integration sites evaluated. At least three randomly chosen non-overlapping unique sets of 300 integrations from the available MGS-PCR sequencing data was assessed. Circles represent the number of total integrations within 10 kbp of another integration site in each group of 300 integrations.

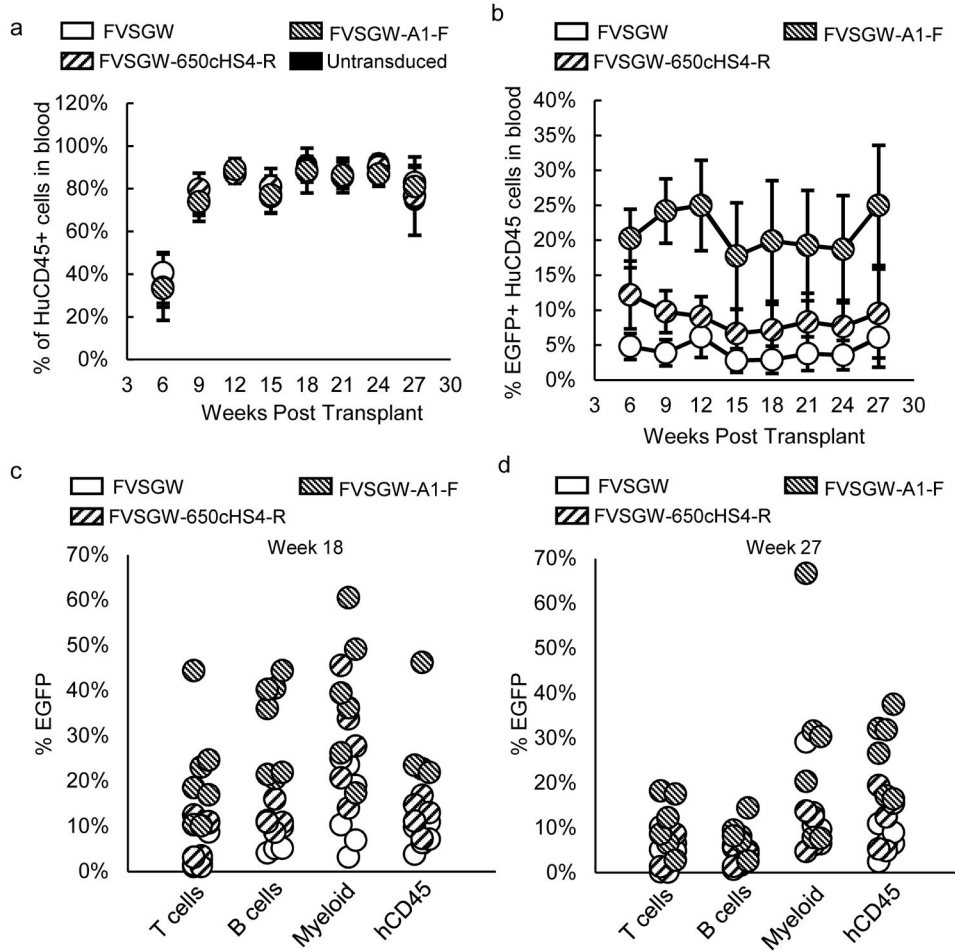


**Figure 3.** Evidence of SCID repopulating cell (SRC) engraftment and hematopoiesis in NSG mice transplanted with transduced human CD34<sup>+</sup> cord blood cells. Peripheral blood was drawn every three weeks and evaluated for the presence of human CD45, mouse CD45, and EGFP expression. Approximate MOI of transplanted HSCs were 6.5, 10, and 17 for FVSGW, FVSGW-650cHS4-R, and FVSGW-A1-F respectively. (a) Evaluation of engraftment efficiency as assessed by the percent of human CD45 of total CD45 expressed on cells in the blood. (b) Retention of vector transduced SRCs as represented by the percent of human CD45 expressing cells which are also expressing EGFP in the peripheral blood. (c and d) Blood was also stained for CD3 (T cells), CD19 (B cells), and CD11b (myeloid). Presented are the percent of the CD45<sup>+</sup>EGFP<sup>+</sup> populations expressing each differentiation marker per mouse. (c) 18 weeks and (d) 27 weeks post-transplant. No significant difference in lineage marking associated with insulated FV vectors. Error bars represent SD.

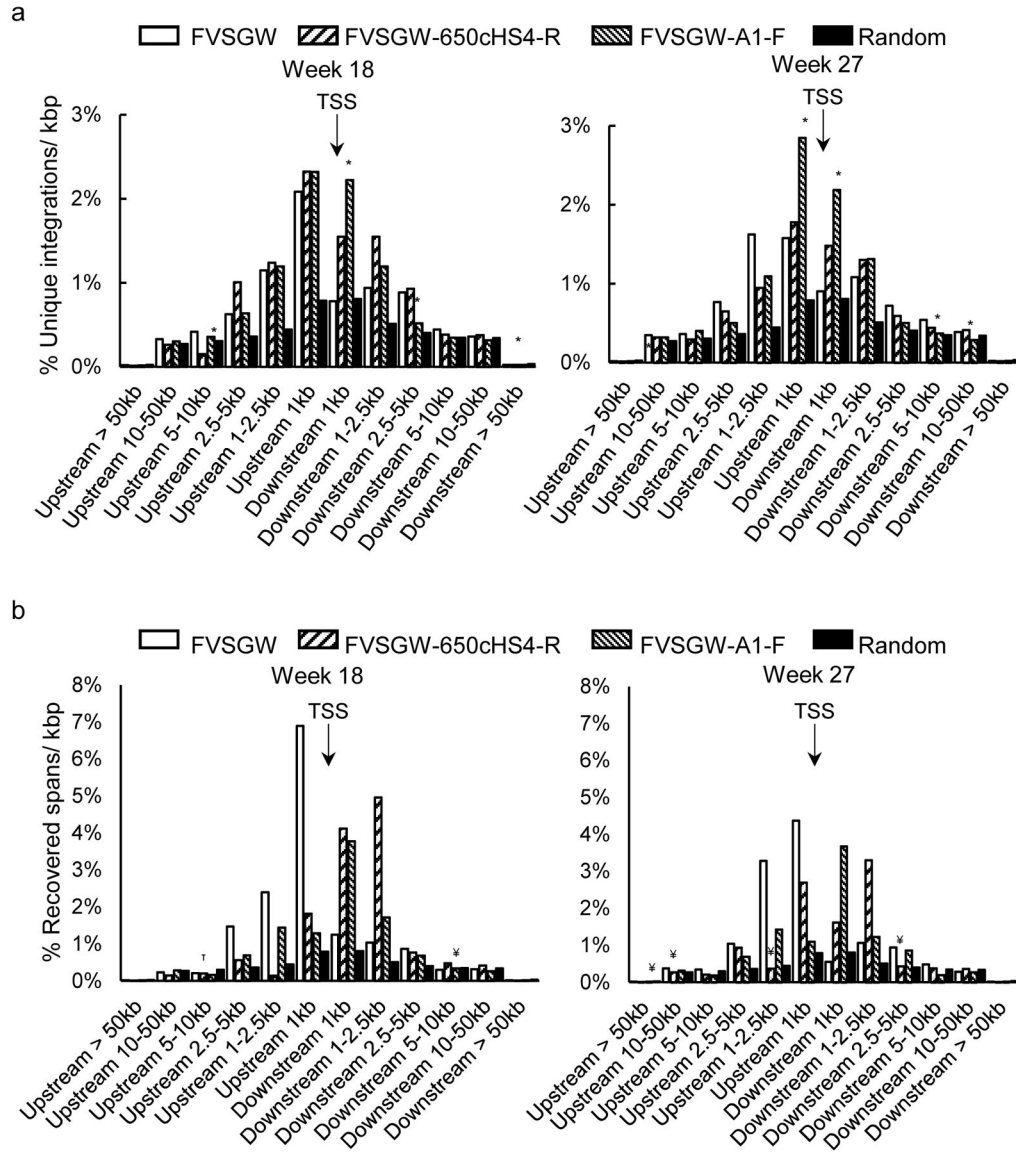


**Figure 4.** Integration profiles of insulated and uninsulated FV vector transduced bone marrow SRCs. (a) Unique integration profile. The positions of unique FV and insulated FV vector integrations in transduced SRCs relative to RefSeq gene transcription start sites (TSS) 18 and 27 weeks post transplantation. At 18 weeks FVSGW, n= 384; FVSGW-650cHS4-R, n= 258; FVSGW-A1-F, n= 1038. At 27 weeks FVSGW, n= 456; FVSGW-650cHS4-R, n= 385; FVSGW-A1-F, n= 913. \*p<0.05 compared to FVSGW. (b) Capture weighted integration profile. The positions of the spans recovered for each unique integration from FV vector and insulated FV vector transduced SRCs relative to RefSeq gene transcription start sites (TSS) 18 and 27 weeks post transplantation. p < 0.05 accept where noted. T, p not significant compared to FVSGW; ¥, p not significant compared to random.

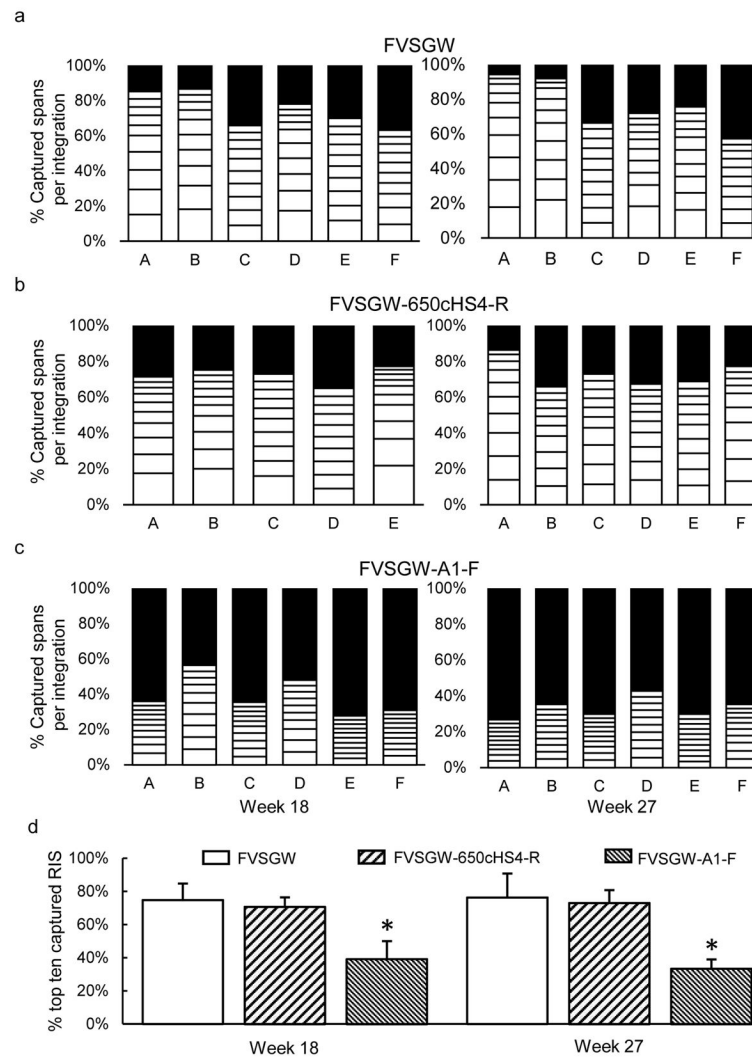


**Figure 5.** Clonality of transduced bone marrow SRCs. The different spans for each unique integration captured from bone marrow was determined. Percent of spans for each captured integration presented. (a) Control FV vector (FVSGW), (b) 650cHS4 insulated FV (FVSGW-650cHS4-R), and (c) A1 insulated FV (FVSGW-A1-F). (d) Contribution of the top ten captured integrants. The average percent of the top ten captured integrants as determined by span is shown. \*p<0.005. Error bars represent SD.



Table 1

Distribution of FV integration sites in transduced human cord blood

	<i>n</i> <sup>a</sup>	In RefSeq gene	Within 50 kbp of RefSeq TSS	In DNase hypersensitivity sites	In proto-oncogene	Within 50 kbp of proto-oncogene TSS
Random	10 000	44.7%	44.4%	1.0%	8.6%	6.5%
FV-control	1 747	41.9%	53.8%	2.5%	8.0%	9.0%
Day 5 FV-cHS4-R	1 200	44.3%	59.0% <sup>b</sup>	2.8%	9.2%	10.3%
FV-AI-F	4 109	41.0%	50.4% <sup>b</sup>	2.4%	7.7%	8.4%
FV-control	1 594	43.0%	53.5%	2.4%	8.8%	7.9%
Day 10 FV-cHS4-R	904	42.5%	59.3% <sup>b</sup>	1.9%	8.2%	9.8% <sup>b</sup>
FV-AI-F	6 489	41.8% <sup>c</sup>	49.0% <sup>b</sup>	1.8%	8.2%	7.6%

TSS, transcription start site; FV, foamy virus; R, reverse orientation; F, forward orientation

<sup>a</sup> *n* the total number of unique integrations<sup>b</sup> significantly different than FV-control, *p*<0.001<sup>c</sup> significantly different than FV-control, *p*<0.05

Table 2

Distribution of unique FV integration sites in transduced SRCs

Week	n	In Genes	Integrations in or near known proto-oncogenes		
			Within 50 kb of TSS	In Proto-oncogenes	Within 50 kb of TSS
18	FV-control	384	44.5%	58.6%	8.6%
	FV-650cHS4-R	258	48.4%	58.1%	8.1%
	FV-A1-F	1 038	41.6%	54.4% <sup>b</sup>	8.1%
27	FV-control	456	47.5%	62.8%	10.1%
	FV-650cHS4-R	385	45.1%	59.3%	11.0%
	FV-A1-F	913	38.6% <sup>b</sup>	54.4% <sup>a</sup>	8.0% <sup>c</sup>

<sup>a</sup> significantly different than FV-control, p<0.001<sup>b</sup> significantly different than FV-control, p<0.01<sup>c</sup> significantly different than FV-control, p<0.05

**Table 3**

Proto-oncogenes near highest captured integrations

Vector	Proto-oncogenes captured at weeks 18 and 27	% contribution 18/27	Distance (bp)	Description
FV-control	CXCL1	18.2/21.9	24 127	C-X-C motif chemokine ligand 1
	PCDH7	9.0/18.3	1 316	protocadherin 7
	C15orf65	5.7/3.2	10 717	chromosome 15 open reading frame 65
	SAMD9L	9.5/8.0	827	sterile alpha motif domain containing 9
FV-650HS4-F	MAGED1	7.9/11.1	15 213	melanoma antigen family D1
	UBR1	4.4/5.8	27 170	ubiquitin protein ligase E3 component n-recognition 1
FV-A1-F	ELMO1	3.5/2.9	47 635	engulfment and cell motility 1

Table 4

Distribution of captured integration sites

Week	n	Total Integrations			Integrations in or near known proto-oncogenes		
		In Genes	Within 50 kb of TSS	In proto-oncogenes	Within 50 kb of TSS	Within 50 kb of TSS	Within 50 kb of TSS
18	FV-control	42.9%	60.7%	5.5%	7.4%		
	FV-650cHS4-R	55.2% <sup>a</sup>	59.4%	11.1% <sup>a</sup>	8.3% <sup>b</sup>		
	FV-AI-F	39.2% <sup>a</sup>	53.3% <sup>a</sup>	7.7% <sup>a</sup>	7.3%		
27	FV-control	36.7%	67.2%	3.3%	8.8%		
	FV-650cHS4-R	45.8% <sup>a</sup>	58.9% <sup>a</sup>	10.9% <sup>a</sup>	9.2%		
	FV-AI-F	36% <sup>b</sup>	53.3% <sup>a</sup>	7.3% <sup>a</sup>	6.2% <sup>a</sup>		

<sup>a</sup> significantly different than FV-control, p<0.001<sup>b</sup> significantly different than FV-control, p<0.01